Supporting Information for Spatial source contribution and interannual variation in deposition of dust aerosols over the Chinese Loess Plateau

Ove Haugvaldstad[1,3], Hui Tang[1,2,5], Anu Kaakinen[2], Christine D. Groot Zwaaftink[6], Henrik Grythe[6], Katja Bohm[2,4], Thomas Stevens[4,2]Zhongshi Zhang [7], Frode Stordal[1]

[1]Department of Geosciences, University of Oslo, Norway

[2]Department of Geosciences and Geography, University of Helsinki, Finland

[3]Norwegian Meteorological Institute, Oslo, Norway

[4]Department of Earth Sciences, Uppsala University, Sweden

[5]Finnish Meteorological Institute (FMI), Climate System Research, Helsinki, Finland

[6]Norwegian Institute for Air Research, Kjeller, Norway.

[7]Department of Atmospheric Science, School of Environmental studies, China University of Geoscience, 430074 Wuhan, China.

Contents of this file

Introduction This document contains additional figures that did not make it to the final manuscript. But they are included in the supplement as supporting information for the analysis presented in the manuscript.

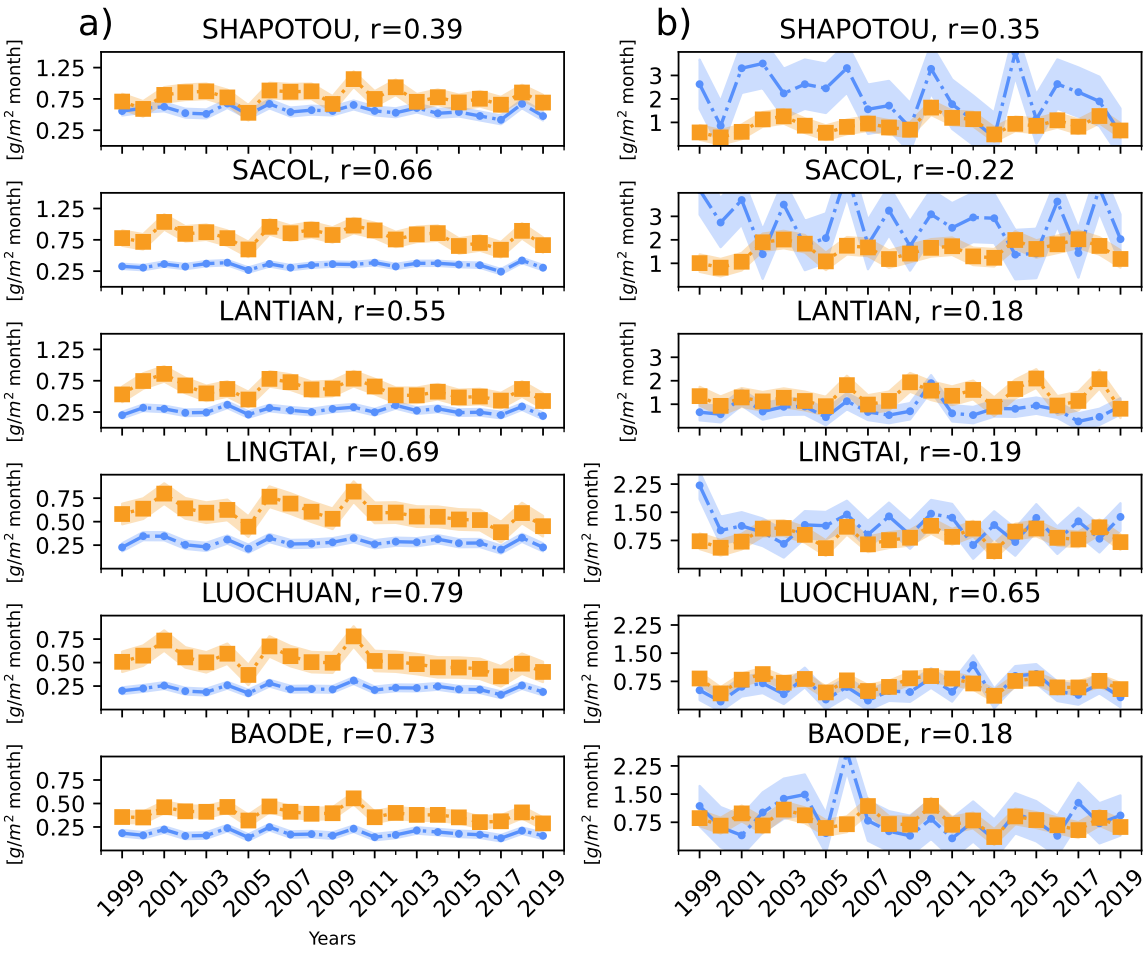

Figure S1. Interannual variation of simulated dry **(a)** and wet **(b)** dust deposition of fine dust at each site, FLEXPART (blue line) MERRA-2 (orange line) (FLEXPART: mean radius 2.057 μm, MERRA-2 dust size bin 2 1.0-1.8 μm). The envelope indicate one standard deviation.

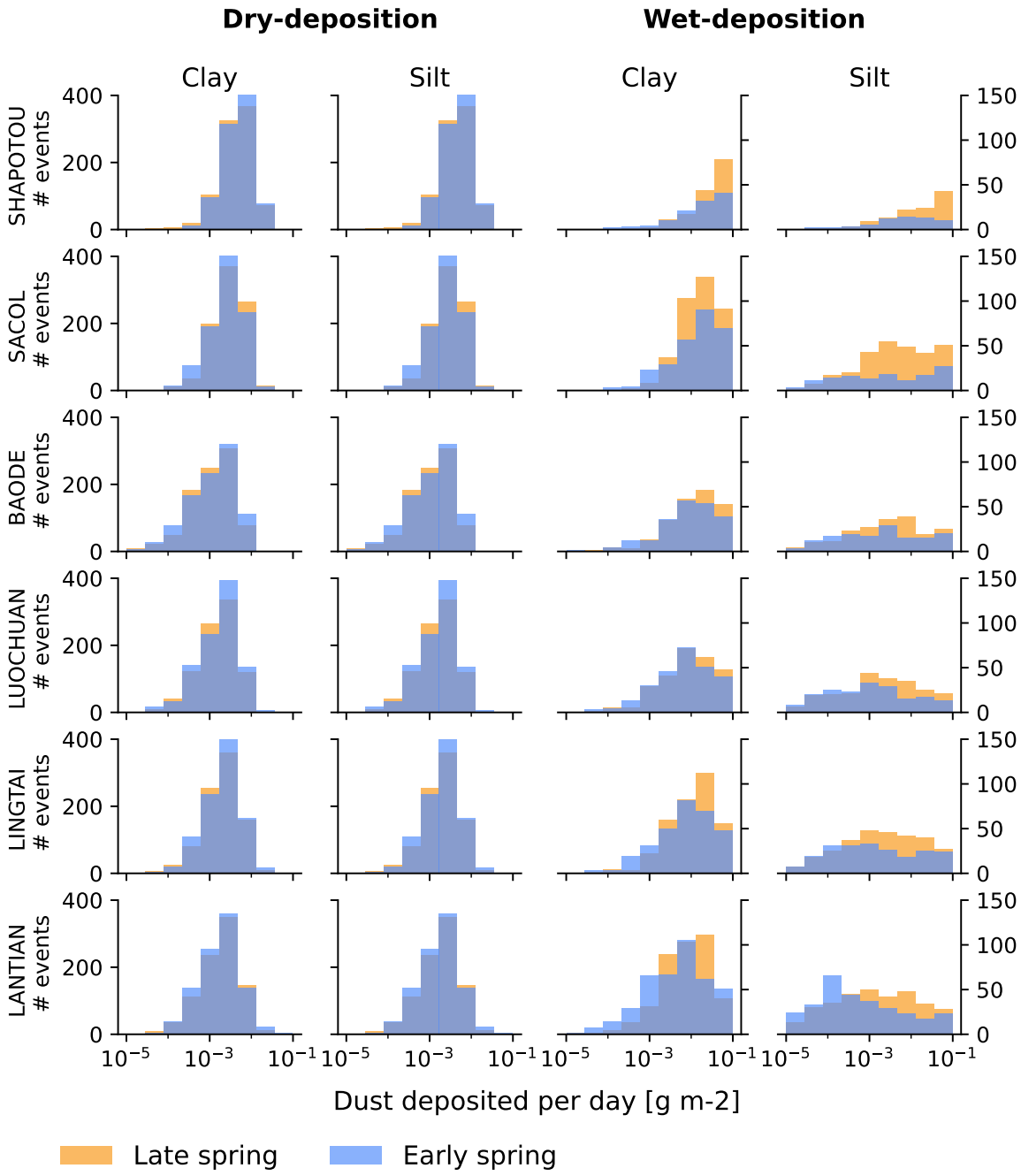

Figure S2. Histogram of daily dry and wet deposited dust for both fine and super-coarse sized dust at the six sites located on the CLP. The spring is split into a late (blue) and early (orange) spring period (late spring after the 15th of April).

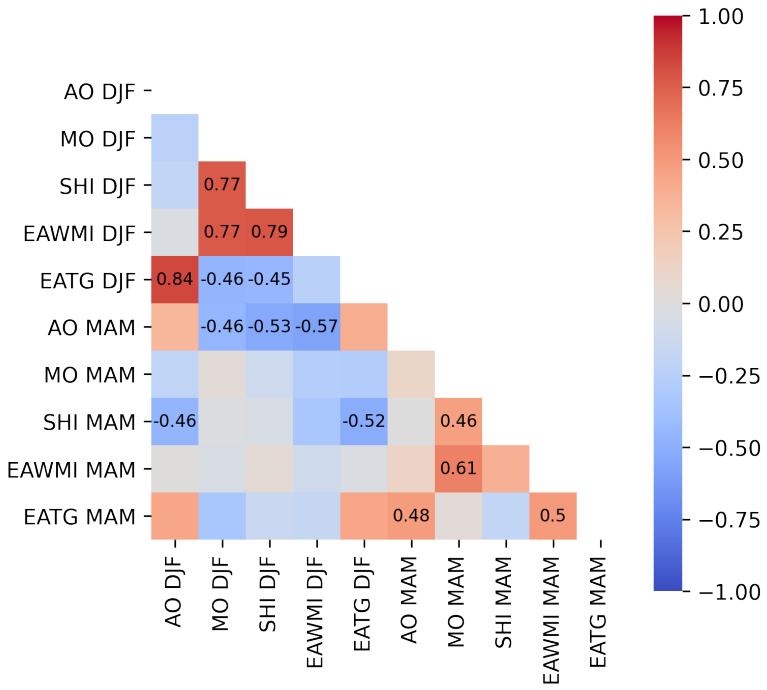

Figure S3. Correlation of circulation indices with each other for winter(December-January-February, DJF) and spring (March-April-May, MAM) . The significant correlations are shown in the figure.

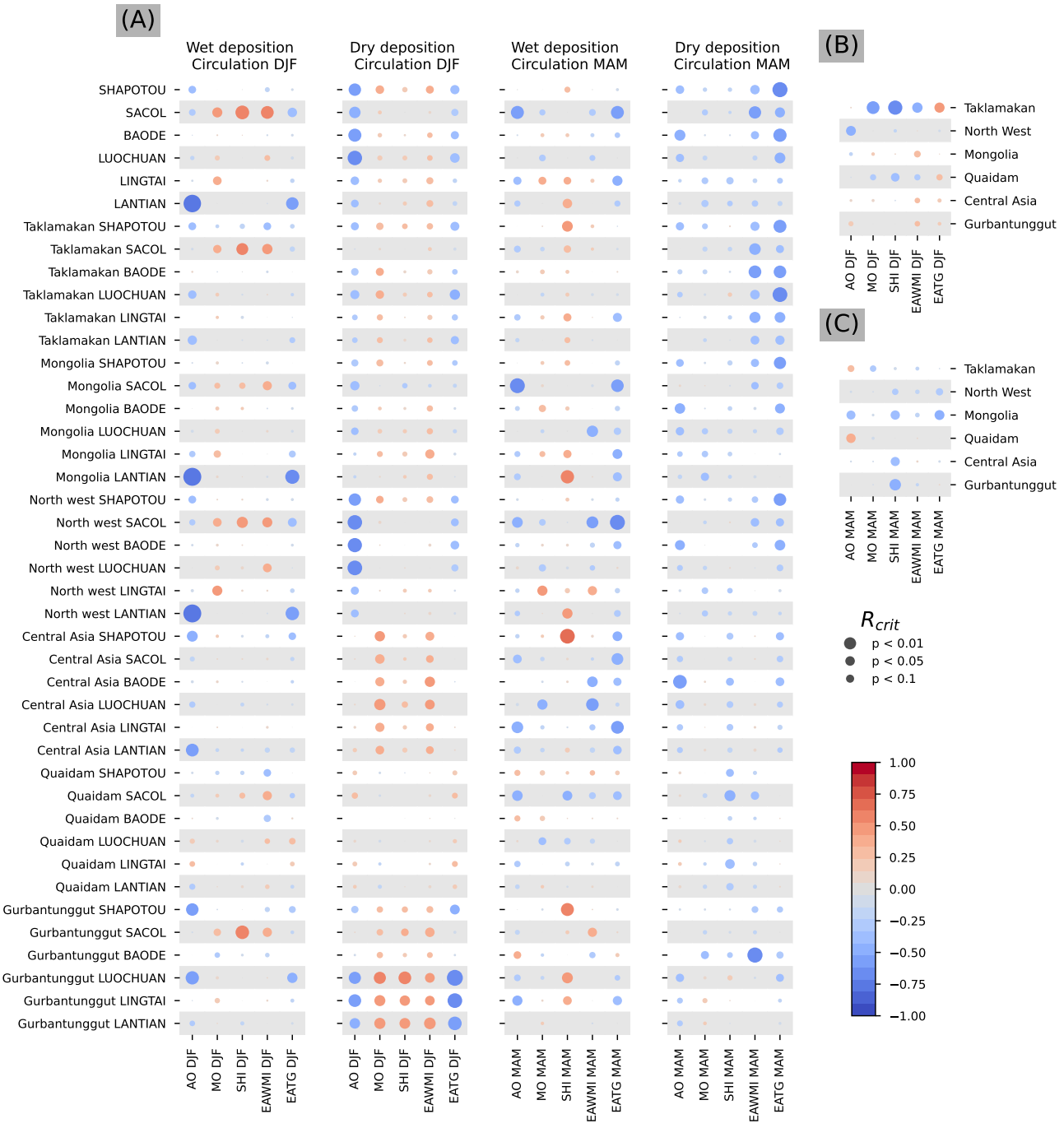

Figure S4. **(A)** Correlations between winter (December-January-February, DJF) and spring (March-April-May, MAM) circulation indices and spring dry- and wet deposition rate of fine dust modeled by FLEXPART, for the whole domain and contributions from individual source regions. **(B-C)** Correlation with dust emissions in the source regions and with winter and spring circulation respectively. The size of the circle indicate the strength of the correlation.

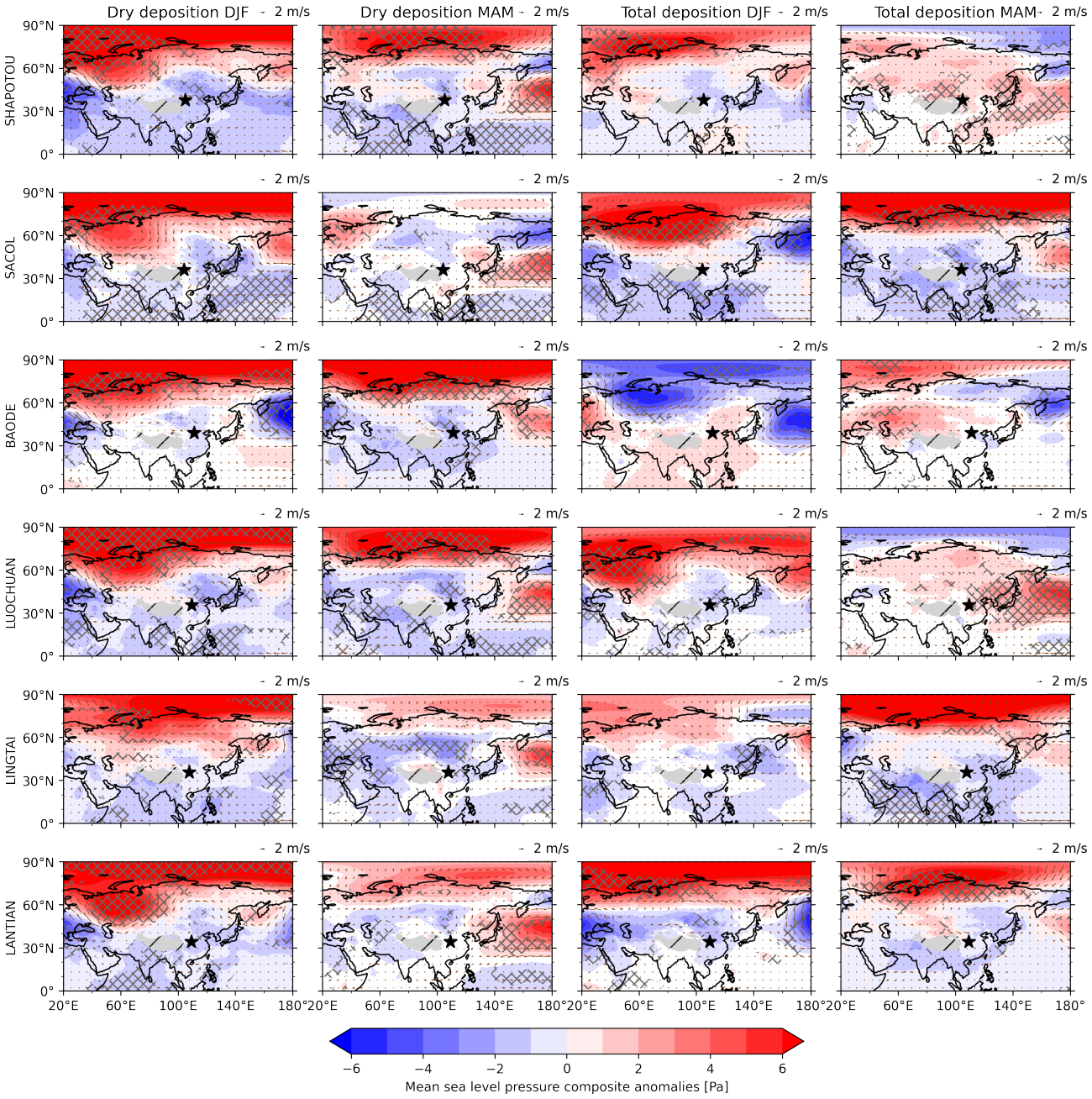

Figure S5. Composite of anomalies based on the difference between strong and weak dust dry-deposition years for winter (December-January-February, DJF) and spring (March-April-May, MAM) , of mean sea level pressure and 850hPa winds. Hatched areas as significant.

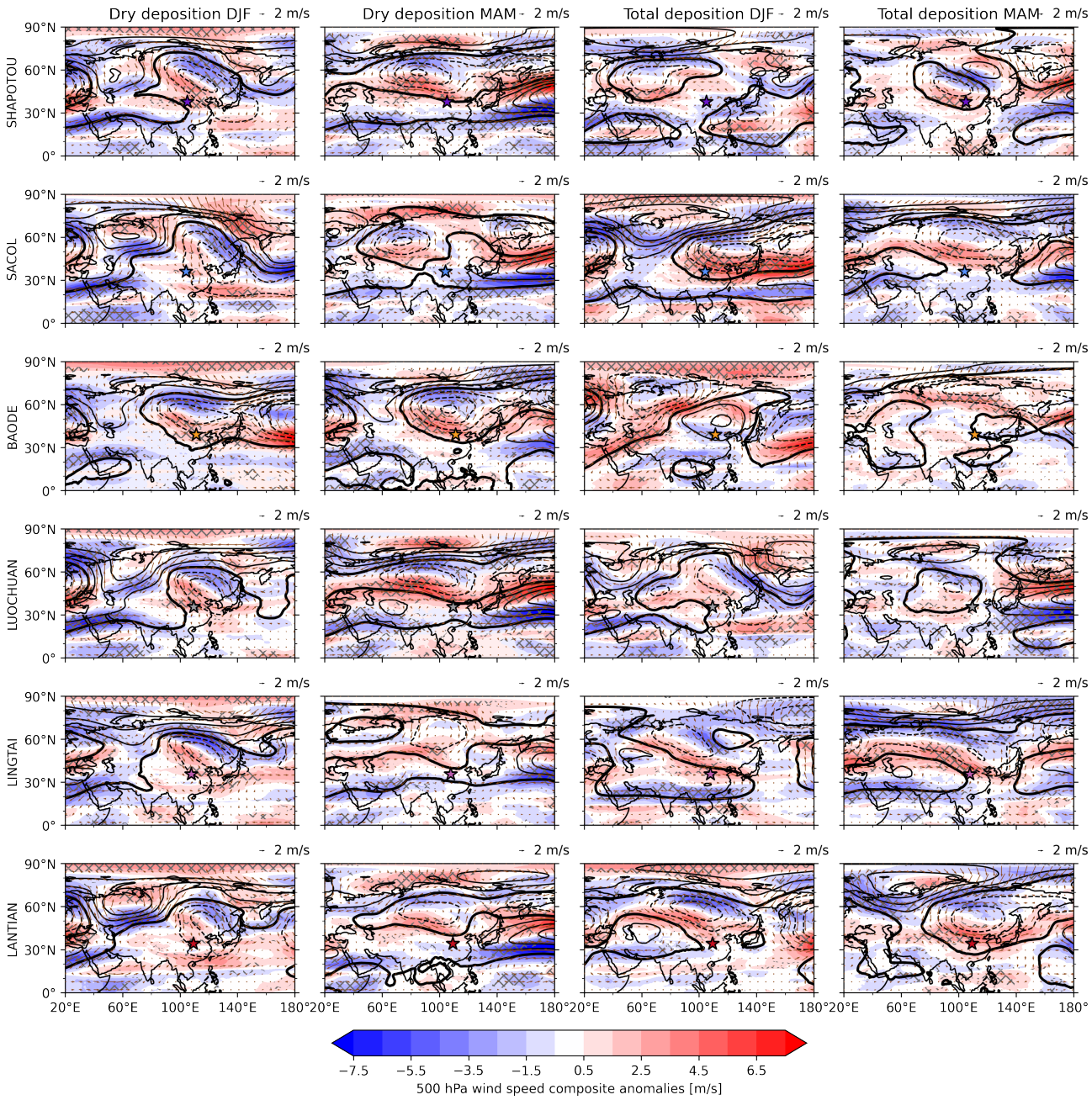

Figure S6. Composite of anomalies based on the difference between strong and weak dust dry-deposition years for winter (December-January-February, DJF) and spring (March-April-May, MAM) , of 500hPa wind speed (shading) and geopotential height (contours, unit dam, distance between contours 2 dam, solid contour are positive anomalies while dotted contours are negative anomalies). The distance be Hatched areas as significant.

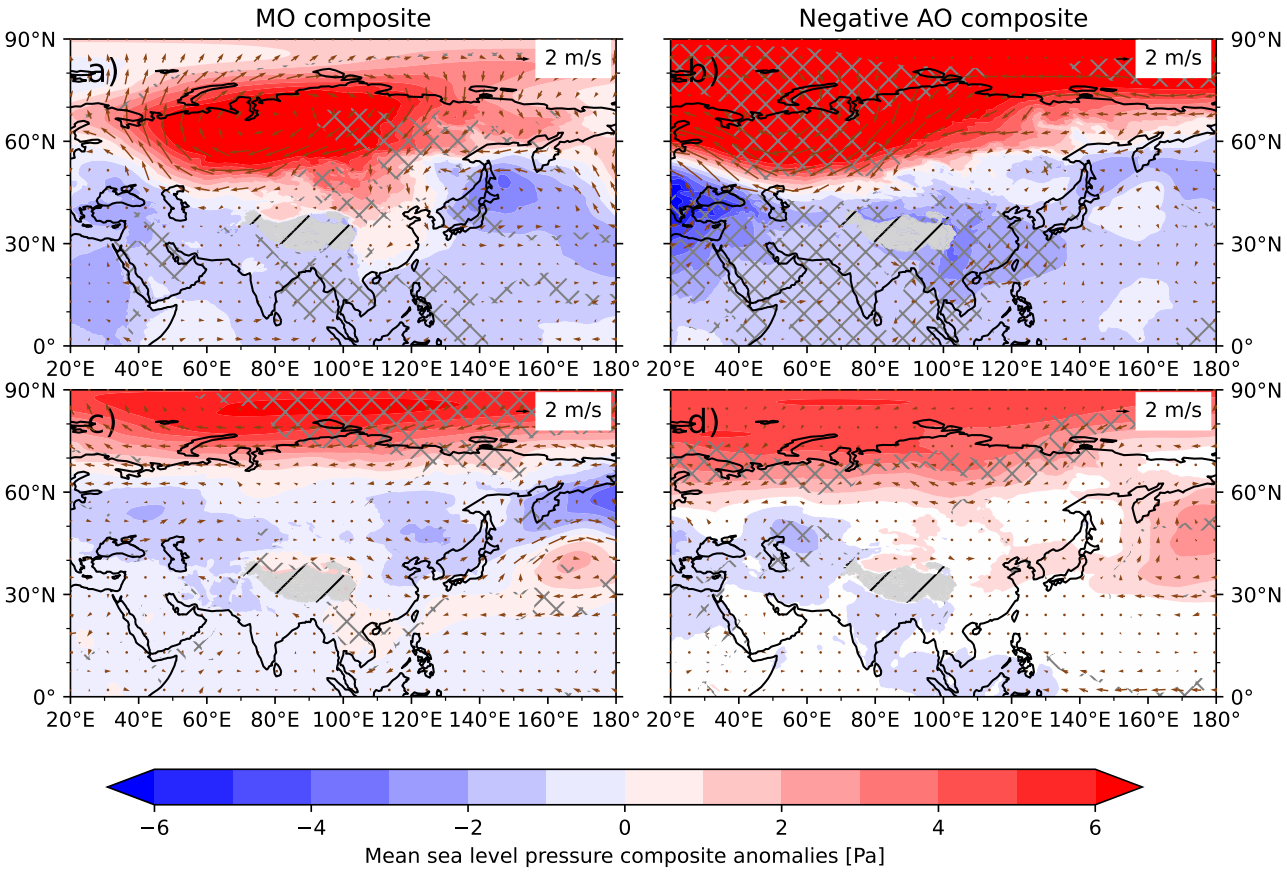

Figure S7. Circulation composite anomalies of 850hPa winds (vectors, unit: m/s) and mean sea level pressure for strong (colored, unit: Pa) - weak winter monsoon years and negative - positive winter AO. (a) and (b) is the DJF anomalies and (c) - (d) is MAM anomalies in the following spring. Data from ERA5.

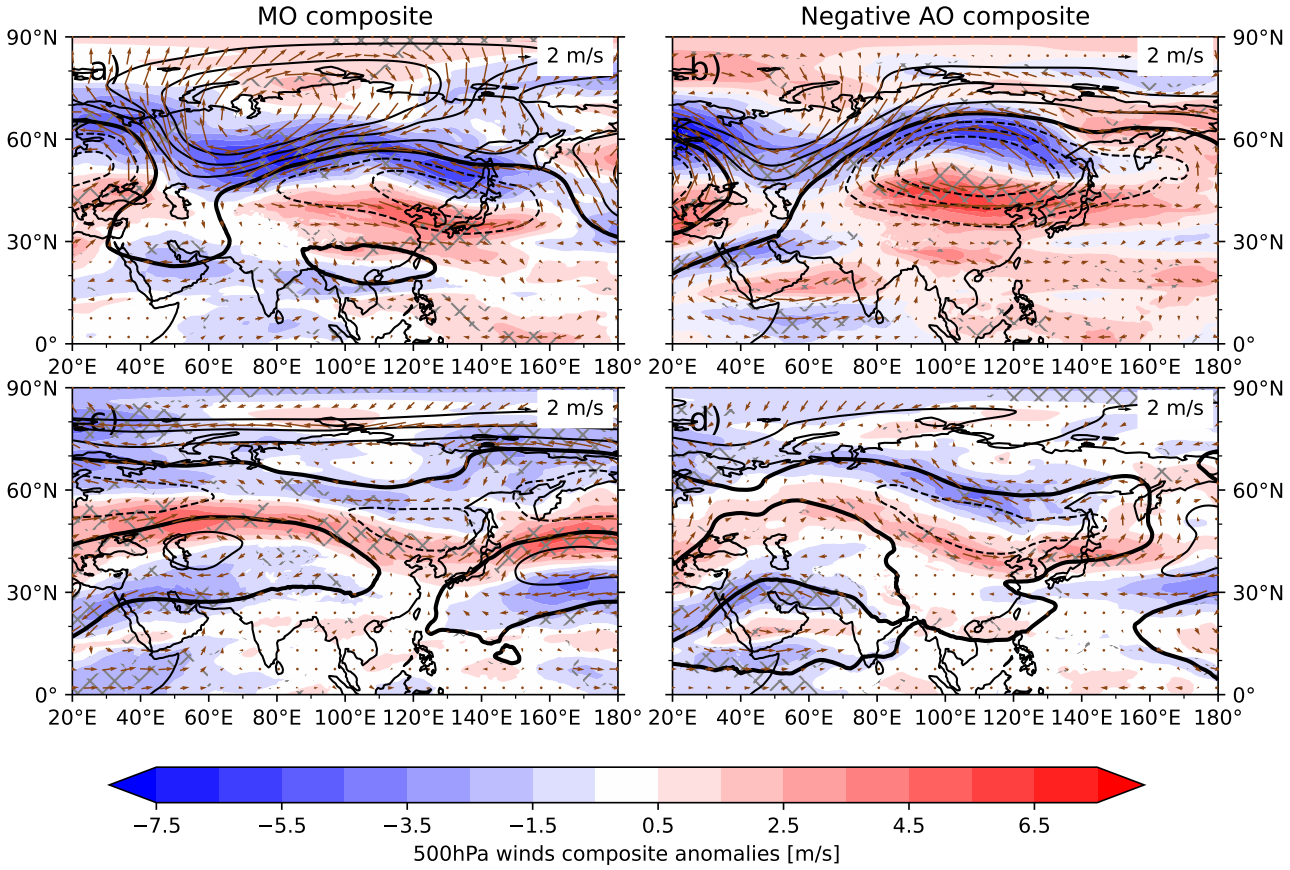

Figure S8. Circulation composite anomalies of 500hPa winds strength (colored, unit m/s), wind direction (vectors, unit m/s) and geopotential height (contours, unit dam, distance between contours 2 dam) for strong - weak winter monsoon years and negative - positive winter AO. (a) and (b) is the DJF anomalies and (c) - (d) is MAM anomalies in the following spring. Data from ERA5.